Micro artificial muscle fiber using NiTi spring for soft robotics

Sangbae Kim*, Elliot Hawkes*, Kyujin Cho†, Matthew Jolda‡, Joe Foley‡ and Robert Wood*
* Harvard Microrobotics Laboratory
Harvard University,
Cambridge, Massachusetts 02139
† Seoul National University
Seoul, South Korea
‡ Government & Industrial Research
iRobot Corporation
Bedford, Massachusetts 01730

***Abstract*—For a new class of soft robotic platforms, development of flexible and robust actuators is quintessential. Remarkable resilience, shape memory effect, high energy density, and scalability are attributed to nickel titanium (NiTi) making it an excellent actuator candidate for meso-scale applications. This paper presents a micro-muscle fiber crafted from shape memory alloy (NiTi) coiled springs. An enhanced spring NiTi model describes the combination of martensite deformation and spring effect due to its geometry. This paper also describes a manufacturing process and characterization for micro-scale NiTi coil actuators in various annealing temperatures. The presented fiber is 400μm in diameter and 0.5m in length exhibiting 50% contraction and 1226J/kg of energy density with 40g of force. By changing the geometry of the spring, force-displacement characteristics can be tuned. An enhanced-performance inverted-spring manufacturing method is also described and characterized. A method of discrete displacement control is presented. Taking advantage of the flexibility of micro-coil spring, we present a novel mesh-worm prototype that utilizes bio-inspired antagonistic actuation for its body deformation and locomotion.**

I. Introduction

Soft robotics is an emerging field that introduces a number of new challenges to roboticists. Soft robots will consist of a flexible body, possess an ability to deform their shape as dictated by various environments, and exhibit superb robustness upon impacts. One of the most challenging elements of such a robot is the soft actuator. Most conventional actuators contain rigid components that limit morphing ability, however a soft actuator can deform along with the surrounding structure.

One of these soft actuators is Nickel Titanium (NiTi) a Shape Memory Alloy (SMA), since its unique martensite transformation makes it inherently flexible. It is also well known for its high energy density, despite its poor efficiency. NiTi has great advantages especially in a small scale where other types of actuators are not available or exhibit poor energy density. The NiTi crystal lattice transforms from the martensite state to the austenite state and produces up to 4% length change as it is heated through the transition temperature range. Some applications require more operating strain to satisfy the dimensional constraints. In order to create larger stroke lengths out of a small lattice structure alteration, NiTi can be restructured into coil springs.

Chang et al.[1], discuss the numerous models for NiTi that has been proposed since the early 1990s. Most of them are thermodynamic models of NiTi wires, tubes, and sheets. Some papers discuss NiTi springs [8], [7], [4], [2], [10], but the models used in these papers are not complete. In this paper, we presents a more complete model that can be used as a design guideline for NiTi spring actuators.

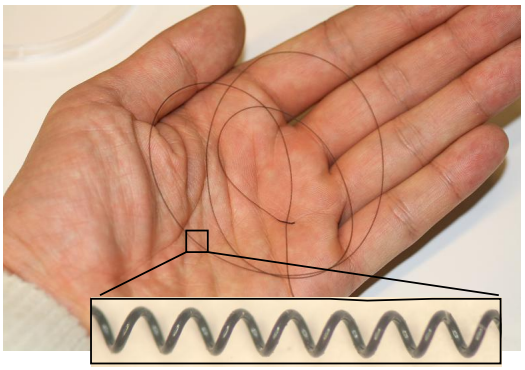

Fig. 1: Fabricated muscle fiber is 400μm in diameter and 0.5m in length.

NiTi coil springs are created from straight wire wound into a coil shape and annealed at a high temperature to reset the 'memorized' shape. The annealing temperature used in the reshaping process affects mechanical properties of NiTi and actuation performance. We present results from experiments to show the variation in properties due to the variation in annealing temperature. These experiments include detwinning force and loaded displacement measurements. After weight-lifting test, springs shows permanent deformation, which is also function of the annealing temperature.

We introduce a manufacturing process of long micro-muscle fibers that enables embedding of artificial muscle fibers into soft structures. The performance of the actuator is dependent not only on the diameter of the coil and wire but also on the pitch of the coil. Methods for altering pitch are presented. Furthermore, we propose and demonstrate a method for creating improved performance NiTi spring actuators by inverting the spring inspired by [6]. A novel method of displacement control

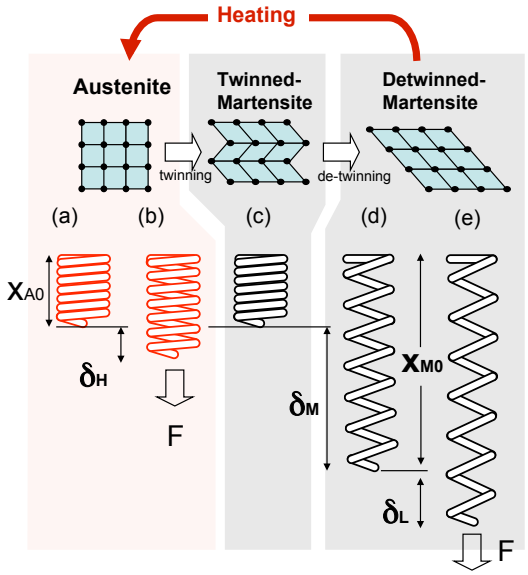

Fig. 2: Five representative states of NiTi spring actuator. (a)-full austenite without load, (b)-full austenite with load, (c)-twinned martensite without load, (d)- fully detwinned martensite without load, (e)-fully detwinned martensite with load.

of NiTi spring is presented. Discrete displacement control is achieved by creating a single wire with segments annealed at different temperatures. Finally, we present a prototype of a robotic worm that consists of flexible mesh tube and micro-coil NiTi fibers. The mesh worm prototype introduces a novel antagonistic actuation scheme inspired by the hydro-stat skeleton structure of Oligochaeta [5].

II. NiTi Spring Actuator Model

Although NiTi spring actuators have been used widely[8], [7], [4], [2], a model of the NiTi spring has not been fully developed. Most papers refer to the mechanical spring equations and use two different shear moduli for the martensite and austenite phases, often denoted as G_M and G_A. But none of the papers discuss the change in the free length of the spring induced by the phase change. The spring elongates to a new free length x_{M0} when in the 100% detwinned martensite phase, compared to a shorter free length x_{A0} in the 100% austenite phase.

The strain of the NiTi spring changes due to two physical phenomena. First is the phase transformation of lattices explained above. Second is the spring effect. The spring extends according to the spring constant, which is a function of various design parameters as well as the phase of the spring. The spring constant in the austenite phase is around 2-3 times larger than in the martensite phase[9].

Figure 2 shows five representative states, which describe the behavior of the spring during actuation. When a spring is heated above the austenite transition temperature without a load, it is contracted fully as shown in Figure 2-(a). When a load F is applied, it elongates by δ_H as shown in Figure 2-(b). When the temperature drops below the transition temperature without load, the crystal lattice twins without noticeable global shape change (Figure 2-(c)). Figure 2-(d) shows a state where the spring is cooled below the martensite transition temperature after a load has detwinned crystal lattice. The free length of the spring increases by δ_M compared to the free length of the spring at the austenite phase. Note that this displacement will occur only after a detwinning force is applied to the spring that has cooled down to a twinned martensite phase. Figure 2-(e) shows the spring at full martensite phase and a load of F being applied. Displacement of δ_L is created with respect to the unloaded fully martensite phase state.

A typical actuation cycle for the NiTi spring would begin with an initial load of F when the actuator is in the martensite phase. Then, the coil is activated to generate a displacement of $\delta_{\text{effective}}$ under a load of F. The effective displacement created by the spring for this case would be

$$\delta_{\text{effective}} = \delta_M + \delta_L - \delta_H \tag{1}$$

where δ is a function of the load, F, spring diameter, D, wire diameter, d, number of active coils in the spring, n and the shear modulus of the spring after annealing, G.

$$\delta = \frac{8FD^3n}{Gd^4} \tag{2}$$

The shear strain of the spring γ is

$$\gamma = \frac{\tau}{G} \tag{3}$$

and the shear stress τ is

$$\tau = \frac{8FD\kappa}{\pi d^3} \tag{4}$$

where κ is a stress correction factor using Wahl's formula [9].

$$\kappa = \frac{4C-1}{4C-4} + \frac{0.615}{C} \tag{5}$$

Spring index C is defined as

$$C = \frac{D}{d} \tag{6}$$

The change in the free length of the spring when the spring changes from austenite phase to martensite phase, δ_M can be calculated from Equation (2) through Equation (6).

$$\delta_M = \frac{\pi\gamma D^2 n}{d\kappa} \tag{7}$$

The shear strain of the spring as it changes from the austenite to martensite phase is approximately 7% [3].

Therefore, for given F, the effective displacement is given as

$$\delta_{\text{effective}} = \frac{\pi\gamma D^2 n}{d\kappa} + \frac{8FD_{\text{eff}}^3 n}{G_M d^4} - \frac{8FD^3 n}{G_A d^4} \tag{8}$$

The coil diameter D is reduced significantly when the spring is extended at the martensite phase. Therefore an effective spring diameter D_{eff} is used for the displacement created by load F.

$$D_{\text{eff}} = D\cos\theta \tag{9}$$

where θ is the angle between the spring wire and the horizontal plane.

III. Experiment and Results

A. Manufacturing NiTi coil and experiment setup

Figure 3 describes a manufacturing method of micro NiTi coil muscle fibers. Core wire (200μm dia.) and NiTi wire (Dynalloy Flexnol (R) 100μm dia.) are clamped at a drill press. A weight is attached at the end of the core wire to keep tension and a ball bearing prevents the weight from turning with the wire, which may cause instability during the winding process. The coil guide is made of a metal tube that can slide on the core wire and a bar attached to the metal tube. The coil guide keeps the coil tightly packed by applying upward forces and cancels the tension from NiTi to keep the core wire vertical.

Once the winding finishes, the end of coil is crimped with the core wire and baked in the furnace at a desired temperature.

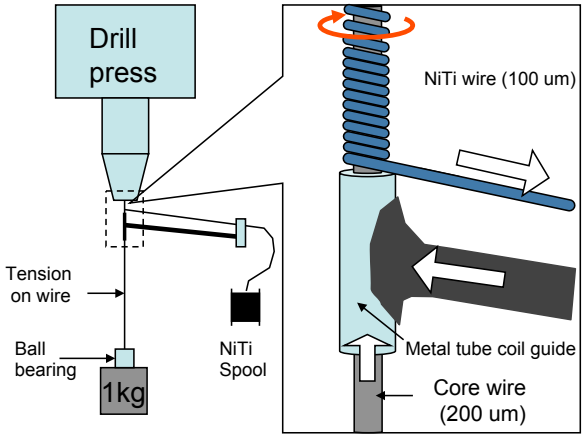

Fig. 3: A simple manufacturing setup enables long strand coiled springs of NiTi muscle fiber. The core wire is under tension and NiTi is wound around the core. The guidance tube is slightly larger than core wire. The tension of NiTi is maintained by friction between the NiTi and the long bar.

B. Effect of annealing temperature

The annealing temperature of the NiTi spring changes various parameters of the spring. From our experiences, we observed inconsistent behaviors in sequential trials possibly due to slip phenomenon at the crystal lattice. However, we were able to identify two noticeable trends that vary with annealing temperatures: (1) the detwinning force decreases as the annealing temperature increases, and (2) springs annealed at high temperatures tend to lose their designed dimensions.

1) Detwinning forces: One of the mechanical characteristics that changes as a function of the annealing temperature is the detwinning force. This affects the work efficiency of the actuator when used in an antagonistic configuration, since the detwinning process requires external work input. NiTi requires a certain amount of force to return to the fully detwinned martensite state through martensite transformation.

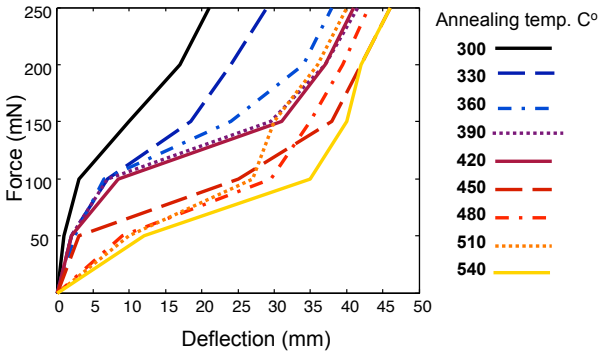

Fig. 4: Deflection of springs annealed at various temperatures under load.

26mm-long NiTi coil springs are annealed at 9 different temperatures ranging from 300°C to 540°C with a 30°C increment. External forces were applied by hanging different weights. To minimize dynamic effects, the weight was applied very slowly, and then, to eliminate spring effect, the weight was removed slowly. The elongated length was measured under no load.

The results are shown in Figure 4. Graphically, the detwinning is shown as the plateau in each curve, similar to a plastic deformation in stress-strain curves. Thus the detwinning force is simply the force at which the plateau occurs. A clear trend is seen as the force decreases with increasing annealing temperature.

2) Permanent deformation of NiTi springs: Figure 5 shows permanently elongated lengths of springs annealed at various temperatures. The deformation represents the difference between the length of a tight 25mm spring and the length of the same spring in the austenite state after lifting a 35g weight. The data shows deformation after one lift. The measured data with springs annealed below 400°C shows reasonable consistency at multiple trials. The springs annealed at temperature higher than 400°C show more deformation after multiple trials. Even though we found that higher annealing temperatures produces lower detwinning forces, for springs annealed above 400°C, the original dimension is lost after a single lifting cycle.

3) Model vs. experiments: Based upon these observations, for the comparison of the model and the experiment in terms of stroke length, we used a spring annealed at 390°C for the weight lifting experiments. Figure 6 shows spring deflection in both the austenite state and the martensite state with various loads. The current used to maintain the spring in the austenite state is 150mA. Predicted values from Equation (2) are plotted

on top of the experiment data. The shear modulus of the NiTi used for the estimated values is calculated through the deflection length in the austenite state because the modulus is also function of annealing temperature. We used a third of austenite shear modulus for martensite shear modulus, which is the typical case of NiTi[9].

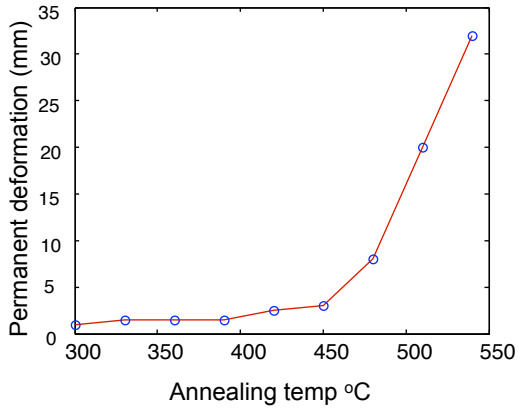

Fig. 5: Permanent plastic deformation after 35g weight lifting experiment.

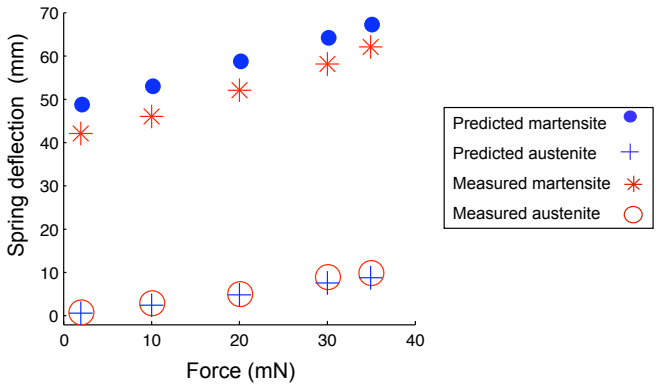

Fig. 6: Comparison between experiment data and model using Equation (8).

C. Energy density

We measured the energy density of the NiTi muscle fiber by measuring work done when it lifts a weight. A 25mm(annealed length) NiTi spring annealed at 390°C lifts a 37.5g weight with stroke length of 50mm. The amount of work is 0.0184J and the weight of the actuator is 0.014g. The measured energy density is 1226J/kg, defined as the amount of work done in a single stroke of the actuator.

D. Tuning of NiTi

The resulting springs behave according to the previously defined equations ((Equation (2)) & (8)). Increasing either the wire diameter or decreasing the diameter of the spring vastly increases the spring stiffness and decreases the displacement.

TABLE I: Stiffness results compared to prediction.

Stretch	**Normalized stiffness** $(\mathrm{kg/s})^2$	**Predicted stiffness** $(\mathrm{kg/s})^2$
1x	38.6	33
2x	64.7	66
3x	99.4	99
4x	128.7	132
5x	173.8	165

Altering these parameters is a very powerful way to modulate spring characteristics, but such power comes at the expense of fine tuning; moving from a 100µmwire to a 150µmwire increases stiffness fivefold (Equation (2)).

A much finer method involves varying the number of coils in a spring, either by altering the length of the spring (using more or fewer coils), or by altering spring coil pitch. To alter pitch, a spring is coiled and annealed at a low temperature ($\approx 300°\mathrm{C}$) to set the shape. Then the coil, while still wrapped around a core wire, is stretched uniformly until the desired pitch is attained. Measurement of pitch is done through total spring length change, and calculated through simple geometry.

Varying the number of coils in a spring by either cutting or pre-stretching is a very practical tuning method. To illustrate, if a 100µm wire spring's stiffness needs to be increased by 10%, it can be achieved by simply pre-stretching 10%, as opposed to finding a new wire with a 105µm diameter, as determined to the Equation (2).

A demonstration of this method produces consistent results as shown in Table I. The G value is approximate.

E. Effect of Inverting SMA Spring

Jee et al.[6] propose a method for creating an "initial tension" or pre-load in a SMA spring actuator by inverting it. This pre-load is valuable for cases which require a compact spring and/or the need to collapse to the initial, unloaded coil length, even in the presence of a load. The traditional method of creating a initial tension on a spring requires twisting the wire while winding. Unfortunately, the shape-setting heat treatment necessary for SMA spring manufacturing relaxes the initial tension, making this method ineffective.

Jee et al.[6] create the initial tension by inverting the spring after the shape-setting treatment is complete. The mechanism for doing this inversion is not described, implying careful bending using pliers. This simplistic method for doing such an inversion is only applicable to springs with a large spring index C and short length. We propose general methods for inverting springs of relatively small spring indexes and long lengths. In addition, we characterize their performance.

The two main inversion methods devised can be seen in Figure 7 & 8. The wrapping method (Figure 7) involves attaching one end of a formed spring to the original core and unwinding it, while re-wrapping it around the core in the opposite direction. This method was easy to perform on springs with large C values, however became impractical on smaller C springs. With the aid of additional tooling, it is possible that this method could produce results, but we chose

to focus our efforts elsewhere.

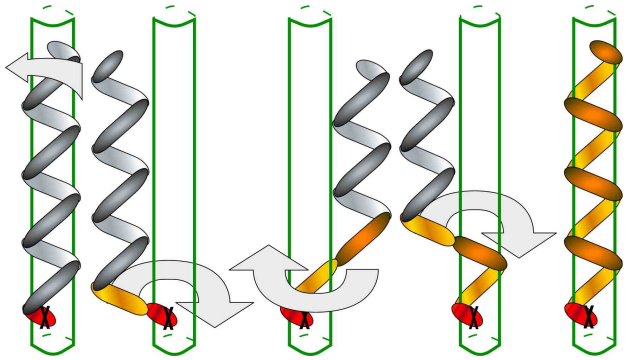

Fig. 7: Inversion of SMA spring by wrapping.

Our favored method, the central tube method (Figure 8), is to pull the spring right through its own center to invert it. To prevent the coils from getting tangled in each other, a thin-walled plastic tube was inserted through the center of the spring which also slightly expands the spring. The springs were initially wound around a core wire and one length of their own winding wire, which was allowed to be used as a center pull as illustrated in Figure 8.

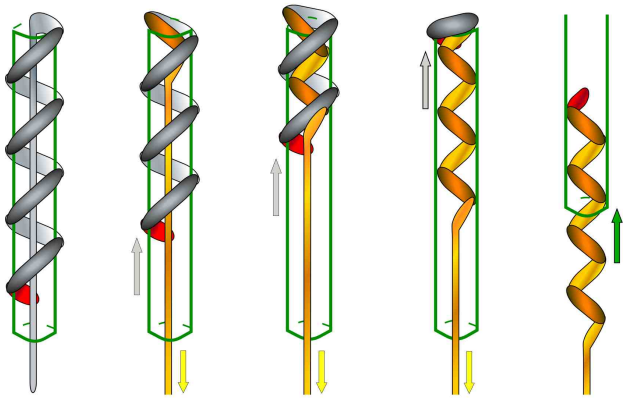

Fig. 8: Inversion of SMA spring using central tube.

We have been successful at using both methods on springs of $C = 20$ and length of 2.5cm. Both methods have produced similar results in spring response. Neither is more advantageous, other than complexity of performing the actual inversion. It should be noted that the original pre-inverted coil should be loosely wound, rather than tightly packed like the original SMA spring actuator design calls for. This is because the spring wishes to return to the originally loose configuration, and therefore will have a quicker response time.

Our testing of the springs has revealed that they have significantly enhanced performance. These tests were performed using 100µm SMA wire wound around a 2032µm core (C = 20). These springs were stretched using a 30g mass and actuated with 6V at 0.55A. Their response time and compression were recorded (Table II). The loose-wound

TABLE II: Performance of normal and inverted SMA springs.

Type	**Wrap**	**Compression** (%)	**Time** (s)
Original	Tight	62	10
Wrap	Loose	77.81	7
Wrap	Tight	70	10.5
Tube	Loose	79.35	8
Tube	Tight	74.36	12

inverted springs respond much faster and are able to retract almost to the minimum length (Figure 9). The only limitation we noticed is that the original un-inverted spring has to be perfectly wound when performing the central tube inversion method. Any imperfection in the winding pattern will cause the spring to tangle itself while in the heated state, and thus not fully returning to the stretched state after cooling.

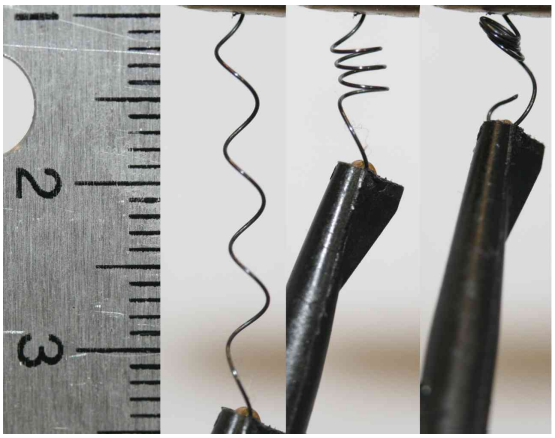

Fig. 9: left) Stretched spring. (center) Original tight-wound spring return. (right) Inverted loose-wound spring return.

F. Discrete control of a series of NiTi springs

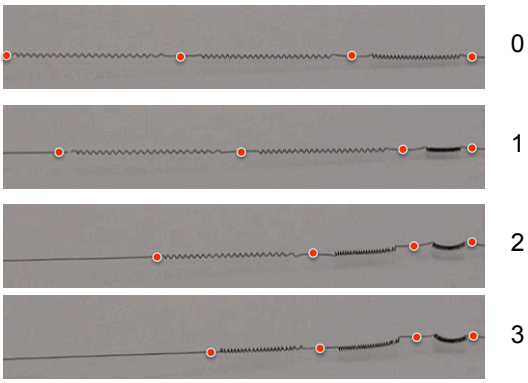

Fig. 10: Each spring segment is annealed at different temperatures and transitions at different current.

NiTi is mostly used as a binary actuator, contracting completely once the phase transition occurs. Some work has been done on controlling the heat input to cause a partial

phase transition and thus control displacement, however such methods are very difficult to control as the inter-phase region is highly nonlinear and very narrow.

We have developed a novel method of displacement control based on altering the transition temperature of discrete sections of the coil. We discovered that annealing two springs at different temperatures has the effect of creating a slightly different transition temperature in each. Thus by annealing a series of coils into a single wire, each at a slightly different annealing temperature, we could create a spring in which each coil contracted at a slightly different input temperature.

Figure 11 shows the input current as a marker of transition temperature of springs annealed at different temperatures.

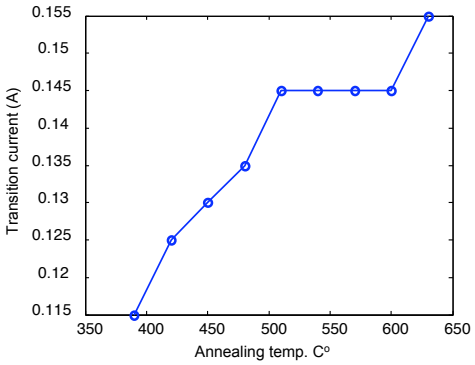

Fig. 11: Transition current varies with annealing temperature.

While the relationship is clearly nonlinear, there is considerable difference in transition temperature such that a number of discrete coils can be made to actuate at discrete input currents. An example is shown in Figure 10, with three coils annealed at 370°C, 480°C, 630°C that exhibit sequential contractions as current is applied.

IV. Prototype

As an application of NiTi muscle fiber, we present a novel antagonistic actuation mechanism, inspired by the hydrostat skeleton structure of Oligochaeta. Figure 12 shows the structure of the prototype and Oligochaeta's muscle groups, which consist of multiple segments. Each segment has both longitudinal muscle and circumferential muscle. As longitudinal muscles contract, the segment shortens in length and increases in diameter. As circumferential muscle contracts, the segment decreases in diameter and increases in length. Utilizing this mechanism, we fabricated a mesh structure with two groups of muscle fibers. A circumferential fiber wraps around the outside of the mesh tube structure, and four longitudinal muscle fibers are attached inside of the tube. The circumferential muscle is divided by two separate electrical connections that can modulate the two segments separately. Four longitudinal muscle fibers are divided into two right muscles and two left muscles that can bend the body in desired directions.

In an antagonistic pair, the active muscles need to provide additional forces that detwin the inactive muscle. Therefore,

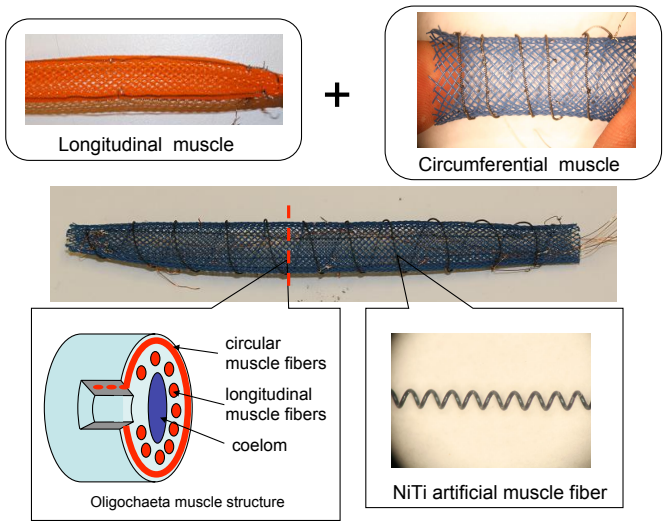

Fig. 12: Earth worm-like prototype and muscle structure of Oligochaeta.

force output is reduced by the detwinning force of the extending antagonistic spring. In the mesh tube structure, the force transmission ratio between the two groups of muscles is dependent upon the mesh angle.

Assuming that the circumferential muscle fiber crosses longitudinal muscle perpendicularly, we can simplify the actuation into a model shown in Figure 13. For example, when circumferential muscle contracts, force equilibrium in longitudinal axis is

$$F_o = F_c \frac{1}{\tan\theta} - F_d \tag{10}$$

where F_o represents the force output in the longitudinal axis, F_c represents the circumferential muscle, and F_d represents the detwinning force of the longitudinal muscle fiber.

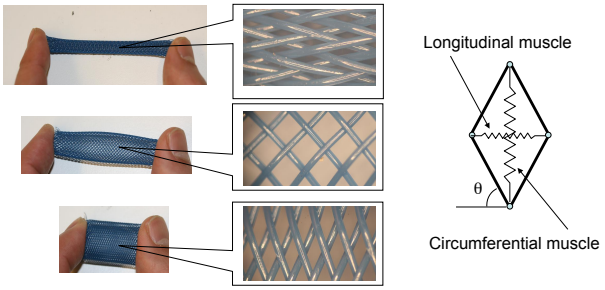

Fig. 13: Fiber direction change in mesh tube according to the deformation of the whole structure and a model that represents the mechanism coupled with two groups of muscle fibers.

Figure 14 describes actuation modes of the prototype. (a)-all longitudinal muscles contract and expand radially. (b)-modular radial contraction by circumferential muscle fiber elongate the corresponding segment. (c)-all circumferential muscles contract and the body reaches maximum length. (d) all muscles are relaxed. (e) and (f)- differential actuation of longitudinal

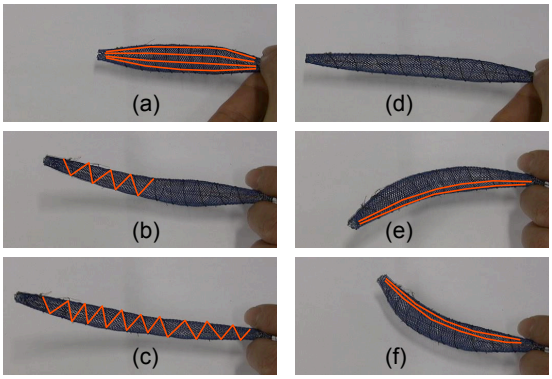

Fig. 14: The action modes of the soft robotic prototype with circumferential actuators and longitudinal actuators. Red lines indicate which muscle groups are activated.

muscles bends the structure and may induce direction change in locomotion.

V. Discussion

A more accurate model of the NiTi spring actuator has been developed that includes the change in free length of the spring due to phase transformation. By using this model, NiTi springs can be finely designed according to the force and displacement requirement. This expands the potential for NiTi spring actuators. Normally, actuators need gears or transmissions to match the impedance of the load, which makes the actuator system bulky. But NiTi spring actuators can be tuned to match the load by changing the shape and the annealing temperature of the spring.

The speed of the actuators varies with electric current that heat the spring above transition temperature. With $150\mathrm{mA}$ of current, the transition takes $1.8\mathrm{s}$.

Another issue, which arises with many artificial muscles, involves the antagonistic actuator. Since NiTi springs are unipolar actuators (there is only a mild bipolar effect), for any repeatable motion, a second antagonistic spring must be used. This limits the stroke length of the active coil, as motion will cease when it has shortened to the point where its output force is equivalent to the detwinning force of actuator in the "off" state. Also, unlike some antagonistic pairs where energy is stored elastically in the "off-state" actuator, NiTi requires work to be done to detwin the passive, martensite spring.

VI. Future work

The future direction of this work is realizing a compliant robotic platform with the NiTi actuators that demonstrate the peristaltic locomotion. Peristaltic locomotion is realized by multiple segments that equipped with antagonistic pair (circumferential and longitudinal muscles). We aim to develop a soft robotic platform that deforms its body dimension significantly and realize locomotion using the body deformation. In order to achieve this goal, multiple segments of the soft body structure that demonstrates axial and radial deformation in this paper with a pattern generator that govern the sequence of each muscle fiber. For efficient peristaltic locomotion, the controller will modulate the sequence of activation of each segment based on the temperature feedback of adjacent actuators. Using multiple longitudinal muscles distributed along the circumference, we plan to develop a robot in capable of steering, overcoming larger obstacles, and searching a gap to go through. For the final goal, we would like to achieve a larger shape change in the body of the robot, such that it could exhibit an exceptional ability to pass through small openings autonomously.

Acknowledgment

This work is supported in part by Defense Advanced Research Projects Agency (DARPA) grant W911NF-08-C-0060 (Chemical Robots).

References

[1] Bi-Chiau Chang, John Shaw, and Mark Iadicola. Thermodynamics of shape memory alloy wire: Modeling, experiments, and application. *Continuum Mechanics and Thermodynamics*, 18(1):83–118, 2006.

[2] K.J. Cho, E. Hawkes, C. Quinn, and R.J. Wood. Design, fabrication and analysis of a body-caudal fin propulsion system for a microrobotic fish. In *Proceedings - IEEE International Conference on Robotics and Automation*, pages 706–711, 2008.

[3] M. Dolce and D. Cardone. Mechanical behaviour of shape memory alloys for seismic applications 1. martensite and austenite niti bars subjected to torsion. *International Journal of Mechanical Sciences*, 43:2631–2656, November 2001.

[4] Y. Dong, Z. Boming, and L. Jun. A changeable aerofoil actuated by shape memory alloy springs. *Materials Science and Engineering A*, 485(1-2):243–250, 2008.

[5] G. Gray. *Animal Locomotion*. W. W. Norton,, New York, 1968.

[6] K. K. Jee, J. H. Han, Y. B. Kim, D. H. Lee, and W. Y. Jang. New method for improving properties of sma coil springs. *The European Physical Journal: Special Topics*, 158:261–266, 2008.

[7] B. Kim, M.G. Lee, Y.P. Lee, Y. Kim, and G. Lee. An earthworm-like micro robot using shape memory alloy actuator. *Sensors and Actuators, A: Physical*, 125(2):429–437, 2006.

[8] Hyo Jik Lee and Jung Ju Lee. Evaluation of the characteristics of a shape memory alloy spring actuator. *Smart Materials and Structures*, 9(6):817–823, 2000.

[9] K. Otsuka and C. M. Wayman. *Shape Memory Materials*. Cambridge University Press, Cambridge, UK, 1998.

[10] Tom C. Waram. *Actuator Design Using Shape Memory Alloys*. T.C. Waram, 1063 King St. W., Suite 204 Hamilton, Ontario L8S 1L8 Canada, second edition, 1993. Phone: (905)525-8251.